The Journal of Agricultural Science

cambridge.org/ags

On solving an isotope dilution model for the partition of phenylalanine and tyrosine uptake by the liver of lactating dairy cows

L. A. Crompton[1], L. L. McKnight[2,3], C. K. Reynolds[1], J. L. Ellis[2], J. Dijkstra[4] and J. France[2]

[1]Department of Animal Sciences, School of Agriculture, Policy and Development, University of Reading, Whiteknights, Reading RG6 6EU, UK; [2]Centre for Nutrition Modelling, Department of Animal Biosciences, University of Guelph, Guelph, Ontario N1G 2W1, Canada; [3]Trouw Nutrition AgResearch Canada, 150 Research Lane, Guelph, ON N1G 4T2, Canada and [4]Animal Nutrition Group, Wageningen University & Research, 6700 AH Wageningen, The Netherlands

Modelling Animal Systems Research Paper

Cite this article: Crompton LA, McKnight LL, Reynolds CK, Ellis JL, Dijkstra J, France J (2022). On solving an isotope dilution model for the partition of phenylalanine and tyrosine uptake by the liver of lactating dairy cows. *The Journal of Agricultural Science* 1–11. https://doi.org/10.1017/S0021859622000442

Received: 9 May 2022
Revised: 9 July 2022
Accepted: 18 July 2022

Key words:
Isotope dilution; kinetic model; liver; phenylalanine; tyrosine

Author for correspondence:
J. France,
E-mail: jfrance@uoguelph.ca

Abstract

An isotope dilution model for partitioning phenylalanine and tyrosine uptake by the liver of the lactating dairy cow is constructed and solved in the steady state. An original ten-pool model is adopted and solved by cleaving it into two five-pool sub-models, one representing phenylalanine and the other tyrosine. If assumptions are made, model solution permits calculation of the rate of phenylalanine and tyrosine uptake from portal vein and hepatic arterial blood supply, hydroxylation, and synthesis and degradation of constitutive protein. The model requires the measurement of plasma flow rate through the liver in combination with amino acid concentrations and plateau isotopic enrichments in arterial and portal and hepatic vein plasma during a constant infusion of [1-^{13}C]phenylalanine and [2,3,5,6-^{2}H]tyrosine tracers. It also requires estimates of the rate of oxidation and protein export secretion. Analysis of measurement errors in experimental enrichments and infusion rates on model solutions indicated that accurate values of the intracellular and extracellular enrichments are central to minimising errors in the calculated flows. Solving the model by cleaving into two five-pool schemes rather than solving the ten-pool scheme directly is preferred as there appears to be less compounding of errors and the results consistently appear to be more biologically feasible. The model provides a means for assessing the impact of hepatic metabolism on amino acid availability to peripheral tissues such as the mammary gland.

Introduction

The overall efficiency of milk protein production relative to dietary nitrogen (N) intake in dairy cows is typically low compared to simple stomach animals at approximately 25–35% (Dijkstra *et al.*, 2013). Not only is there an economic cost to the producer associated with this inefficiency, N losses from livestock production contribute significantly to greenhouse gas emissions and water course and air pollution (Dijkstra *et al.*, 2018; Uwizeye *et al.*, 2020). Milk protein synthesis is sensitive to essential amino acid supply, in particular to group 1 essential amino acids where mammary gland rate of uptake matches output in milk protein, whereas group 2 amino acids have greater flexibility in use for different purposes by the gland (Nichols *et al.*, 2019). Among the group 1 essential amino acids, milk protein synthesis is sensitive to particularly phenylalanine (PHE) when dietary supply is low (Rulquin and Pisulewski, 2000) or as shown by studies where PHE-deficient infusion mixtures were administered (Doepel *et al.*, 2016). In the post-absorptive state, the liver is the major site of PHE metabolism and catabolism and as such net removal from portal vein and hepatic arterial blood typically accounts for substantial proportions of the net absorption of PHE by the portal-drained viscera (Reynolds, 2002, 2006). The liver balances supply from absorption and demand from peripheral tissues.

Several *in vivo* studies have examined the net flow of PHE across the liver of dairy cows using arterio-venous difference techniques (Hristov *et al.*, 2019) and reported a negative measurement (e.g. Raggio *et al.*, 2007; Cantalapiedra-Hijar *et al.*, 2014; Larsen *et al.*, 2015), suggesting the liver is a major site of PHE utilization. In general, PHE has two metabolic fates, incorporation into protein or conversion to tyrosine (TYR) via PHE hydroxylase (oxidation). PHE catabolism, as a result, follows the pathway of TYR catabolism. Therefore, the simultaneous infusion of PHE and TYR stable isotope tracers is preferred when examining PHE metabolism experimentally, and mathematical models are needed to resolve the kinetic data generated by such isotope infusion studies.

In a previous publication (Crompton *et al.*, 2018), we presented a ten-pool compartmental model describing PHE and TYR metabolism in the liver of lactating dairy cows. The model

describes the partitioning of PHE and TYR between constitutive and export protein synthesis and other metabolic fates such as hydroxylation of PHE to TYR. It was solved in the steady state as a single integrated model, i.e. as one set of simultaneous algebraic equations. Initial solutions to the model for each cow were found to be infeasible, i.e. some flows had negative values and were therefore non-physiological. Therefore, error bands of ±25% were placed around the values of any prescribed intracellular enrichments and any measured extracellular enrichments close to minimum detection levels, and the solution space mapped out by these bands was searched to find the best feasible solution for each cow. This best feasible solution was obtained using a sum of squares minimization procedure (Crompton *et al.*, 2018). The present study is a progression of this work and our previous model of leucine metabolism in the bovine liver (France *et al.*, 1999). The objective herein was to investigate an alternative approach to solving the ten-pool PHE-TYR model. The approach involves cleaving the model at the PHE hydroxylation flow to create two five-pool sub-models (one for PHE and one for TYR), then solving the two sub-models sequentially (first PHE then TYR) and linking the two solutions algebraically to re-create an integrated model solution. A similar cleaving approach was recently applied successfully to an eight-pool model of the mammary gland for the same amino acids (Crompton *et al.*, 2022).

The model

Overall scheme

The scheme adopted is shown in Fig. 1. It contains four intracellular and six extracellular pools. The intracellular pools are free PHE (pool 6), PHE in export protein (pool 5), free TYR (pool 7) and TYR in export protein (pool 8), while the extracellular ones represent portal vein PHE and TYR (pools 1 and 3), hepatic artery PHE and TYR (pools 2 and 4) and hepatic vein PHE and TYR (pools 9 and *X*, where *X* represents the Roman numeral ten). The flows of PHE and TYR between pools and into and out of the system are shown as arrowed lines. The export protein-bound PHE pool has a single inflow: from free PHE, F_{56}, and two outflows: secretion of export protein, F_{05}, and degradation, F_{65}. The intracellular free PHE pool has four inflows: from the degradation of constitutive liver protein, F_{60}, from the extracellular portal vein pool, F_{61}, from the hepatic artery pool, F_{62}, and from degradation of export protein, F_{65}. The pool has four outflows: synthesis of constitutive liver protein, F_{06}, incorporation into export protein, F_{56}, hydroxylation to the intracellular free TYR pool, F_{76}, and outflow to the extracellular hepatic vein PHE pool, F_{96}. The intracellular free TYR pool has five inflows: from the degradation of constitutive liver protein, F_{70}, from the extracellular portal vein TYR pool, F_{73}, from the hepatic artery TYR pool, F_{74}, from the intracellular PHE pool, F_{76}, and from the degradation of export protein, F_{78}. The pool has four outflows: oxidation and TYR degradation products, $F_{07}^{(o)}$, synthesis of constitutive liver protein, $F_{07}^{(s)}$, incorporation into export protein, F_{87}, and outflow to the extracellular hepatic vein TYR pool, F_{X7}. The export protein-bound TYR pool has one inflow: from the intracellular free TYR pool, F_{87}, and two outflows: secretion of export protein, F_{08}, and degradation, F_{78}. The extracellular portal vein PHE pool has a single inflow: entry into the pool, F_{10}, and two outflows: uptake by the liver, F_{61}, and release into the extracellular hepatic vein PHE pool, F_{91}. The extracellular hepatic artery PHE pool has a single inflow: entry into the pool, F_{20}, and two outflows: uptake by the liver, F_{62}, and release into the extracellular hepatic vein PHE pool, F_{92}. The same description applies to the corresponding TYR pools, i.e. pools 3 and 4 with flows F_{30}, F_{73}, F_{X3}, F_{40}, F_{74} and F_{X4}, respectively. The extracellular hepatic vein PHE pool has three inflows: bypass from the portal vein PHE pool, F_{91}, bypass from the hepatic artery PHE pool, F_{92}, and release from the intracellular PHE pool, F_{96}, and one outflow out of the system, F_{09}. The same description applies to the corresponding TYR pool with flows F_{X3}, F_{X4}, F_{X7} and F_{0X} respectively.

As noted above, this scheme can be solved as a ten-pool model (Crompton *et al.*, 2018). Alternatively, it can also be solved by decomposing it into two five-pool schemes (i.e. a PHE sub-model and a TYR sub-model), then linking the two schemes. The PHE and TYR sub-models are both similar structurally to the model of LEU kinetics presented by France *et al.* (1999). In the present study, labelled [1-^{13}C]PHE and [2,3,5,6-^{2}H]TYR were infused into the jugular vein at a constant rate, and enrichment in several pools were measured.

PHE sub-model

The schemes adopted for the movement of total and labelled PHE in the PHE sub-model are shown in Figs 2(*a*) and (*b*) respectively. The fundamental equations are (mathematical notation is defined in Table 1):

$$\frac{dQ_1}{dt} = F_{10} - F_{61} - F_{91} \quad (1)$$

$$\frac{dQ_2}{dt} = F_{20} - F_{62} - F_{92} \quad (2)$$

$$\frac{dQ_5}{dt} = F_{56} - F_{05} - F_{65} \quad (3)$$

$$\frac{dQ_6}{dt} = F_{60} + F_{61} + F_{62} + F_{65} - F_{06} - F_{56} - F_{76} - F_{96} \quad (4)$$

$$\frac{dQ_9}{dt} = F_{91} + F_{92} + F_{96} - F_{09} \quad (5)$$

and for [1-^{13}C] PHE:

$$\frac{dq_1}{dt} = I_1 - e_1(F_{61} + F_{91}) \quad (6)$$

$$\frac{dq_2}{dt} = I_2 - e_2(F_{62} + F_{92}) \quad (7)$$

$$\frac{dq_5}{dt} = e_6F_{56} - e_5(F_{05} + F_{65}) \quad (8)$$

$$\frac{dq_6}{dt} = e_1F_{61} + e_2F_{62} + e_5F_{65} - e_6(F_{06} + F_{56} + F_{76} + F_{96}) \quad (9)$$

$$\frac{dq_9}{dt} = e_1F_{91} + e_2F_{92} + e_6F_{96} - e_9F_{09} \quad (10)$$

https://doi.org/10.1017/S0021859622000442 Published online by Cambridge University Press

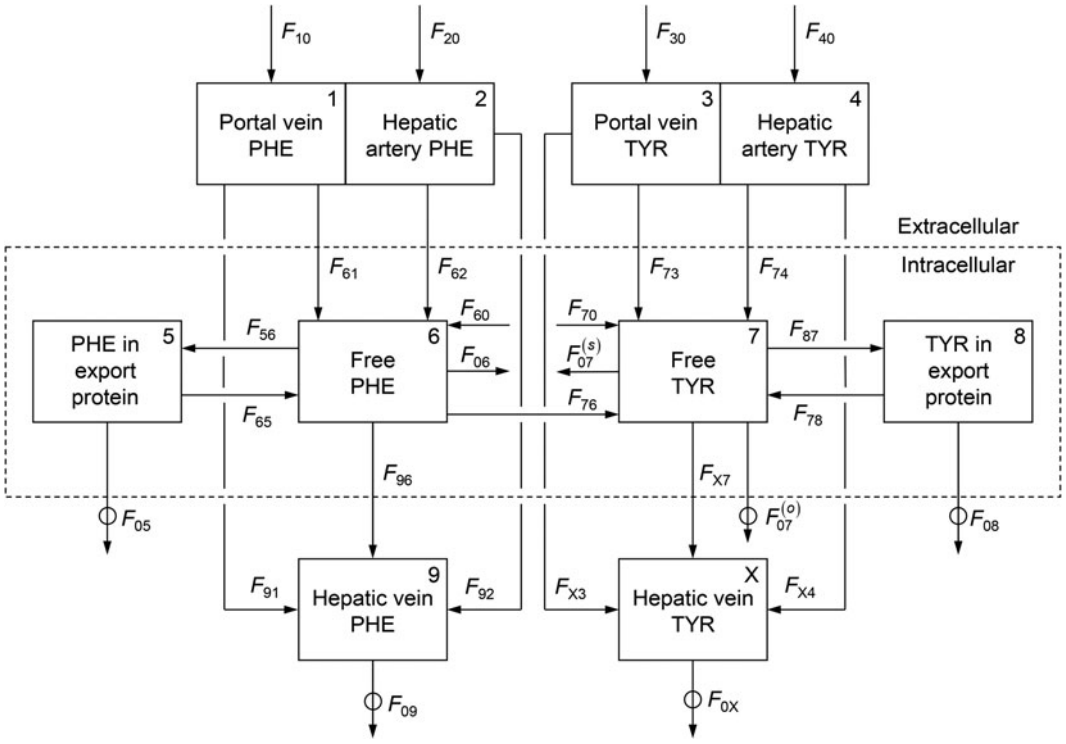

Fig. 1. Scheme for the uptake and utilization of PHE and TYR by the liver of lactating dairy cows as described by Crompton *et al*. (2018). The small circles in Fig. 1 indicate flows out of the system which need to be measured experimentally.

When the system is in steady state with respect to both total and labelled PHE, the derivative terms in these ten differential equations are zero. For the scheme assumed, the enrichment of the intracellular protein-bound pool equalizes with that of the free pool as steady state is approached (i.e. $e_5 = e_6$). After equating intracellular enrichments and eliminating redundant equations, the five differential equations for labelled PHE, Eqns (6)–(10), yield the following four identities:

$$I_1 - e_1(F_{61} + F_{91}) = 0 \tag{11}$$

$$I_2 - e_2(F_{62} + F_{92}) = 0 \tag{12}$$

$$e_1F_{61} + e_2F_{62} - e_6(F_{06} + F_{56} + F_{76} + F_{96} - F_{65}) = 0 \tag{13}$$

$$e_1F_{91} + e_2F_{92} + e_6F_{96} - e_9F_{09} = 0 \tag{14}$$

To obtain steady-state solutions to the sub-model, it is assumed that PHE secreted in export protein and its removal from the hepatic vein pool (i.e. F_{05} and F_{09}, respectively) can be measured experimentally. Further, it is mathematically convenient (and physiologically acceptable) to assume that percentage PHE extraction by the liver is the same from the portal vein and hepatic artery supplies, giving:

$$\frac{F_{91}}{F_{92}}\left(=\frac{F_{61}}{F_{62}}\right) = \frac{F_{10}}{F_{20}} \tag{15}$$

Algebraic manipulation of Eqns (1)–(5) with the derivatives set to zero, together with Eqns (11)–(15), gives:

$$F_{10} = I_1/e_1 \tag{16}$$

$$F_{20} = I_2/e_2 \tag{17}$$

$$\overline{F_{56} - F_{65}} = \tilde{F}_{05} \tag{18}$$

$$F_{91} = \frac{(e_9 - e_6)\tilde{F}_{09}}{(e_1 - e_6) + (e_2 - e_6)\dfrac{F_{20}}{F_{10}}} \tag{19}$$

$$F_{92} = \frac{F_{20}}{F_{10}}F_{91} \tag{20}$$

$$F_{96} = \tilde{F}_{09} - F_{91} - F_{92} \tag{21}$$

$$F_{61} = F_{10} - F_{91} \tag{22}$$

$$F_{62} = F_{20} - F_{92} \tag{23}$$

$$\overline{F_{06} + F_{76}} = \frac{e_1}{e_6}F_{61} + \frac{e_2}{e_6}F_{62} - \overline{F_{56} - F_{65}} - F_{96} \tag{24}$$

https://doi.org/10.1017/S0021859622000442 Published online by Cambridge University Press

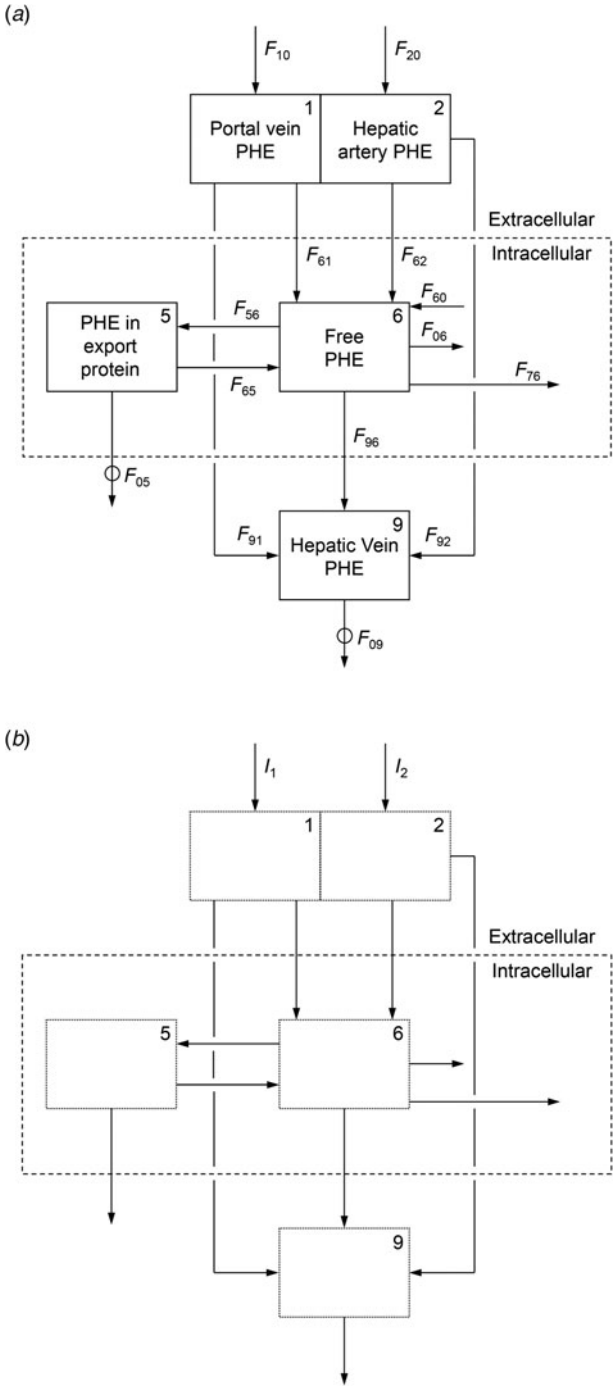

Fig. 2. Scheme for the uptake and utilization of PHE by the liver of lactating dairy cows: (a) total PHE, (b) [^{13}C] labelled PHE. The small circles in Fig. 2(*a*) indicate flows out of the system which need to be measured experimentally.

$$F_{60} = \overline{F_{06} + F_{76}} + \overline{F_{56} - F_{65}} + F_{96} - F_{61} - F_{62} \tag{25}$$

where for these equations the italics denote steady-state values of flows and enrichments, the tilde identifies a measured flow, and the over-lining indicates coupled flows (which cannot be separately estimated within the model). The coupled flow $\overline{F_{06} + F_{76}}$ is separated when the sub-models are linked back together.

Table 1. Principle symbols used for the kinetic model

F_{ij}	Flow of PHE[a] or TYR[a] to pool *i* from *j*; F_{i0} denotes an external flow into pool *i* and F_{0j} denotes a flow from pool *j* out of the system	μmol/min
I_i	Effective rate of constant infusion of ^{13}C labelled PHE into primary pool *i*	μmol/min
Φ_i	Effective rate of constant infusion of ^{2}H labelled TYR into primary pool *i*	μmol/min
Q_i	Quantity of PHE[a] or TYR[a] in pool *i*	μmol
q_i	Quantity of ^{13}C labelled PHE in pool *i*	μmol
ϕ_i	Quantity of ^{2}H labelled TYR in pool *i*	μmol
e_i	Enrichment of ^{13}C PHE in pool *i*: ($= q_i/Q_i$)	molar % excess/μmol
ε_i	Enrichment of ^{2}H TYR in pool *i*: ($= \phi_i/Q_i$)	molar % excess/μmol
t	Time	min

[a]Total material (i.e. tracee + tracer).

TYR sub-model

The schemes adopted for the movement of total and labelled TYR in the TYR sub-model are shown in Figs 3(*a*) and (*b*) respectively. The fundamental equations are:

$$\frac{dQ_3}{dt} = F_{30} - F_{73} - F_{X3} \tag{26}$$

$$\frac{dQ_4}{dt} = F_{40} - F_{74} - F_{X4} \tag{27}$$

$$\frac{dQ_7}{dt} = F_{70} + F_{73} + F_{74} + F_{76} + F_{78} - F_{07}^{(o)} - F_{07}^{(s)} - F_{87} - F_{X7} \tag{28}$$

$$\frac{dQ_8}{dt} = F_{87} - F_{08} - F_{78} \tag{29}$$

$$\frac{dQ_X}{dt} = F_{X3} + F_{X4} + F_{X7} - F_{0X} \tag{30}$$

and for [2,3,5,6-^{2}H]TYR:

$$\frac{d\phi_3}{dt} = \Phi_3 - \varepsilon_3(F_{73} + F_{X3}) \tag{31}$$

$$\frac{d\phi_4}{dt} = \Phi_4 - \varepsilon_4(F_{74} + F_{X4}) \tag{32}$$

$$\frac{d\phi_7}{dt} = \varepsilon_3 F_{73} + \varepsilon_4 F_{74} + \varepsilon_8 F_{78} - \varepsilon_7(F_{07}^{(o)} + F_{07}^{(s)} + F_{87} + F_{X7}) \tag{33}$$

https://doi.org/10.1017/S0021859622000442 Published online by Cambridge University Press

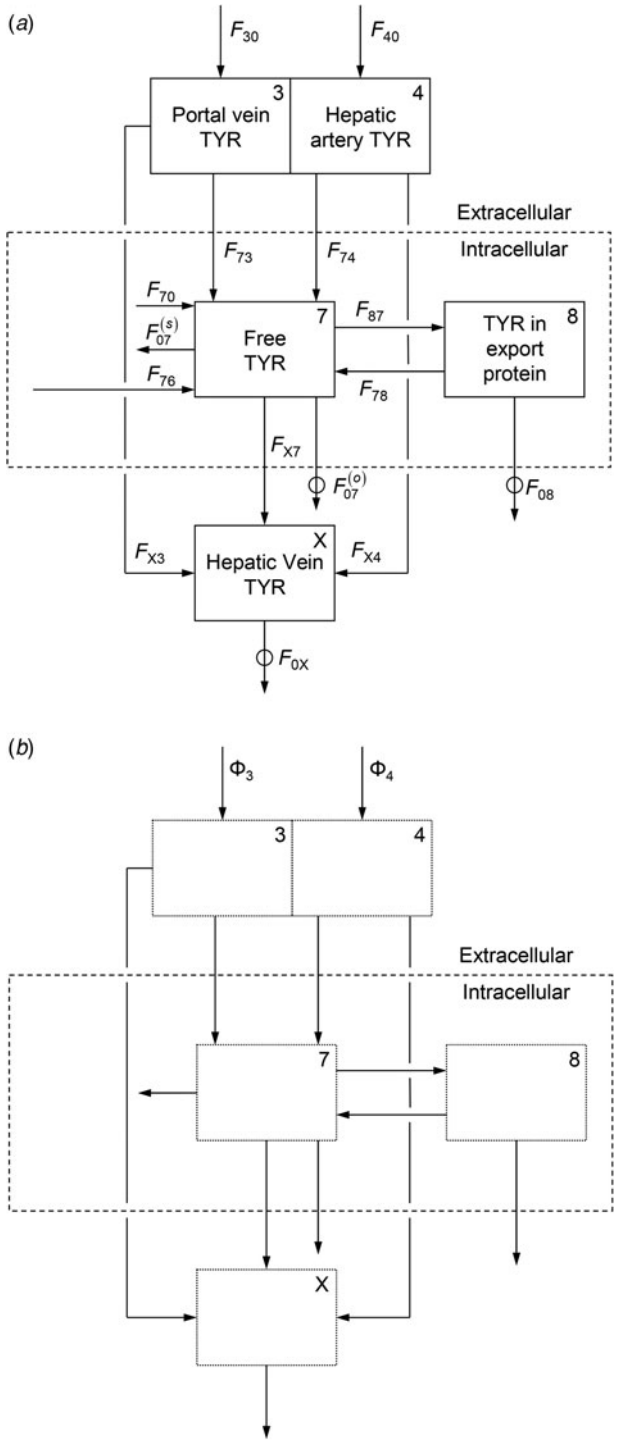

Fig. 3. Scheme for the uptake and utilization of TYR by the liver of lactating dairy cows: (a) total TYR, (b) [^{2}H] labelled TYR. The small circles in Fig. 3(*a*) indicate flows out of the system which need to be measured experimentally.

$$\frac{d\phi_8}{dt} = \varepsilon_7 F_{87} - \varepsilon_8(F_{08} + F_{78}) \tag{34}$$

$$\frac{d\phi_X}{dt} = \varepsilon_3 F_{X3} + \varepsilon_4 F_{X4} + \varepsilon_7 F_{X7} - \varepsilon_X F_{0X} \tag{35}$$

When the system is in steady state with respect to both total and labelled TYR, the derivative terms in these ten differential equations are zero. For the scheme assumed, the enrichment of the intracellular protein-bound pool equalizes with that of the free pool as steady state is approached (i.e. $\varepsilon_7 = \varepsilon_8$). After equating intracellular enrichments and eliminating redundant equations, the five differential equations for labelled TYR, Eqns (31)–(35), yield the following four identities:

$$\Phi_3 - \varepsilon_3(F_{73} + F_{X3}) = 0 \tag{36}$$

$$\Phi_4 - \varepsilon_4(F_{74} + F_{X4}) = 0 \tag{37}$$

$$\varepsilon_3 F_{73} + \varepsilon_4 F_{74} - \varepsilon_7(F_{07}^{(o)} + F_{07}^{(s)} + F_{87} + F_{X7} - F_{78}) = 0 \tag{38}$$

$$\varepsilon_3 F_{X3} + \varepsilon_4 F_{X4} + \varepsilon_7 F_{X7} - \varepsilon_X F_{0X} = 0 \tag{39}$$

To obtain steady-state solutions to the sub-model, it is assumed that oxidation, TYR secreted in export protein and its removal from the hepatic vein pool (i.e. $F_{07}^{(o)}$, F_{08} and F_{0X}, respectively) can be measured experimentally. Further, it is mathematically convenient to assume that percentage TYR extraction by the liver is the same from the portal vein and hepatic artery supplies, giving:

$$\frac{F_{X3}}{F_{X4}}\left(= \frac{F_{73}}{F_{74}}\right) = \frac{F_{30}}{F_{40}} \tag{40}$$

Algebraic manipulation of Eqns (26)–(30) with the derivatives set to zero, together with Eqns (36)–(40), gives:

$$F_{30} = \Phi_3/\varepsilon_3 \tag{41}$$

$$F_{40} = \Phi_4/\varepsilon_4 \tag{42}$$

$$\overline{F_{87} - F_{78}} = \tilde{F}_{08} \tag{43}$$

$$F_{X3} = \frac{(\varepsilon_X - \varepsilon_7)\tilde{F}_{0X}}{(\varepsilon_3 - \varepsilon_7) + (\varepsilon_4 - \varepsilon_7)\dfrac{F_{40}}{F_{30}}} \tag{44}$$

$$F_{X4} = \frac{F_{40}}{F_{30}} F_{X3} \tag{45}$$

$$F_{X7} = \tilde{F}_{0X} - F_{X3} - F_{X4} \tag{46}$$

$$F_{73} = F_{30} - F_{X3} \tag{47}$$

$$F_{74} = F_{40} - F_{X4} \tag{48}$$

https://doi.org/10.1017/S0021859622000442 Published online by Cambridge University Press

$$F_{07}^{(s)} = \frac{\varepsilon_3}{\varepsilon_7} F_{73} + \frac{\varepsilon_4}{\varepsilon_7} F_{74} - \tilde{F}_{07}^{(o)} - \overline{F_{87} - F_{78}} - F_{X7} \quad (49)$$

$$\overline{F_{70} + F_{76}} = \tilde{F}_{07}^{(o)} + F_{07}^{(s)} + \overline{F_{87} - F_{78}} + F_{X7} - F_{73} - F_{74} \quad (50)$$

where for these equations the italics denote steady-state values of flows and enrichments, the tilde identifies a measured flow, and the over-lining indicates coupled flows (which cannot be separately estimated). The coupled flow $\overline{F_{70} + F_{76}}$ is separated when the sub-models are linked back together.

Linking the PHE and TYR sub-models

The two sub-models can be linked by considering constitutive liver protein. Assuming a fixed protein composition for constitutive liver tissue, then the ratios of TYR to PHE in protein synthesized and protein degraded (μmol TYR/μmol PHE) are equal:

$$\frac{F_{70}}{F_{60}} = \frac{F_{07}^{(s)}}{F_{06}} \quad (51)$$

This assumption allows Eqns (24) and (50) to be uncoupled. Differencing these coupled flows:

$$\overline{F_{06} + F_{76}} - \overline{F_{70} + F_{76}} = F_{06} - F_{70} = b \quad (52)$$

Using Eqn (51) to substitute for F_{70} in the above equation:

$$F_{06} - \frac{F_{60} F_{07}^{(s)}}{F_{06}} = b$$

$$[F_{06}]^2 - bF_{06} - F_{60} F_{07}^{(s)} = 0$$

Solving this quadratic:

$$F_{06} = \frac{b + \sqrt{b^2 + 4F_{60} F_{07}^{(s)}}}{2} \quad (53)$$

Note that only positive roots of this quadratic are permissible, so any negative roots must be discarded. Therefore:

$$F_{70} = F_{06} - b \quad (54)$$

$$F_{76} = \overline{F_{06} + F_{76}} - F_{06} \quad (55)$$

The overall scheme can now be solved by computing Eqns (16)–(25), (41)–(50) and (52)–(55) sequentially.

Application

Application of the model is illustrated using data from experiments conducted at the University of Reading in the UK with multi-catheterized Holstein-Friesian dairy cows (Hanigan *et al.*, 2004). In the study herein, animals were in mid-lactation (average live-weight 656 kg) fed total mixed ration (TMR) diets consisting of a 50:50 mixture on a dry matter (DM) basis of forage and concentrate with the forage comprised of grass silage and chopped dried Lucerne in a 25:75 ratio on a DM basis. Concentrates were formulated to provide crude protein levels of approximately 110 and 200 g/kg concentrate DM, such that average TMR crude protein concentration were 128 and 175 g/kg DM. Diets were fed hourly using automatic feeders to establish pseudo-steady state. The average daily DM intake and milk yield for the four animals were 21.8 kg/d and 30.5 litres/d, respectively. The cows were given constant abomasal infusions of water (18 litres/d) for 4 d, followed by a buffered mixture of essential amino acids for a further 6 d, administered at a daily rate equivalent to the essential amino acids in 800 g milk protein. On the last day of each water or essential amino acid infusion period, the animals received a primed, continuous jugular vein infusion of [1-^{13}C] PHE (350 mg/h) and [2,3,5,6-^{2}H]TYR (100 mg/h) in sterile saline at a constant rate for 8 h. Throughout the infusion, hourly sets of blood samples were taken simultaneously from catheters in the dorsal aorta and the portal and hepatic veins for the measurement of blood flow rate (by dye dilution) and nutrient metabolism by the portal drained viscera and liver. The steady-state values used for model inputs were the average of the final four blood samples taken 5–8 h after the infusion started.

The relevant experimental measurements are given in Table 2. They are reported for three animals during the amino acid infusion (1 low protein diet; 2 high protein) and one animal during the water infusion (high protein diet). They are based on plasma rather than whole blood values. PHE and TYR measurements are based on free rather than total (i.e. free plus bound) plasma PHE and TYR. The effective isotope infusion rates to the liver, I_1, I_2 and Φ_3, Φ_4, were obtained from portal vein and arterial concentration and enrichment of PHE and TYR and plasma flow rate in the portal vein and hepatic artery. The flows F_{09} and F_{0X} were determined from hepatic vein PHE and TYR concentration and plasma flow rate in the hepatic vein. The intracellular enrichments e_6 and ε_7 and the flows F_{05} and F_{08} were not measured experimentally and had to be prescribed. Unpublished observations from our laboratories demonstrated an intracellular to extracellular enrichment ratio of 0.3 ($n = 4$; SD 0.07; range 0.19–0.38) for PHE and TYR. Therefore, the missing intracellular free PHE and TYR enrichments, e_6 and ε_7 were calculated as 0.3 times the corresponding arterial enrichments e_2 and ε_4 respectively. The export protein flows F_{05} and F_{08} were assigned values of 33.8 μmol/min and 25.0 μmol/min respectively based on Raggio *et al.* (2007) and the relative proportion of PHE and TYR in bovine serum albumin as a representative export protein (UniProt Consortium, 2017). The flow $F_{07}^{(o)}$ was obtained from labelled CO_2 elevation in plasma flow across the liver and hepatic vein PHE enrichment (Harris *et al.*, 1992). Calculated flows are presented in Table 2.

The solutions to the split model described herein are shown in Table 3. All initial calculated flows were biologically feasible, in contrast to when the model was solved as an integrated ten-pool scheme (Crompton *et al.*, 2018). Combining input data reported herein and those reported by Crompton *et al.* (2018) enabled comparison of the solutions from the two five-pool schemes with corresponding solutions obtained using the integrated ten-pool model (Crompton *et al.*, 2018). The averaged flows from both models are shown in Table 4 and highlight some major differences in the values of the flows emanating from the

https://doi.org/10.1017/S0021859622000442 Published online by Cambridge University Press

Table 2. Experimental and other inputs

Cow	323/16[a]	341/31	341/32[a]	6132/48[a]
Dietary CP (g/kg DM)	175	175	175	128
Milk yield (litre/d)	40.2	27.6	28.0	26.0
Plateau Enrichment (molar % excess)				
e_1	1.84	1.13	1.94	2.10
e_2	3.04	1.81	3.15	3.22
e_6	0.91	0.54	0.95	0.97
e_9	1.82	1.26	2.11	2.06
ε_3	0.82	0.32	0.79	0.81
ε_4	1.13	0.50	1.29	1.15
ε_7	0.34	0.15	0.39	0.35
ε_X	0.74	0.33	0.83	0.74
Flow (μmol/min)				
I_1	61.5	19.9	58.9	64.8
I_2	6.93	14.6	43.3	12.1
Φ_3	22.6	4.88	13.7	16.7
Φ_4	2.30	3.52	10.3	3.16
F_{05}	33.8	33.8	33.8	33.8
$F_{07}^{(o)}$	650	339	572	413
F_{08}	25.0	25.0	25.0	25.0
F_{09}	2901	2274	3473	2781
F_{0X}	2543	2040	2115	2039

CP, crude protein.
[a]Essential amino acid infusion.

Table 3. Phenylalanine and tyrosine uptake and partition by the liver for four lactating dairy cows obtained using the two five-pool models (symbols are defined in the text and Table 1)

Cow	323/16	341/31	341/32	6132/48
Flow (μmol/min)				
F_{10}	3349	1768	3042	3090
F_{20}	228	804	1375	377
$\overline{F_{56} - F_{65}}$	33.8	33.8	33.8	33.8
F_{91}	2455	1400	2030	2159
F_{92}	167	636	917	263
F_{96}	279	237	526	359
F_{61}	894	368	1012	930
F_{62}	60.9	167	458	113
F_{60}	1051	787	2131	1356
F_{30}	2767	1513	1730	2064
F_{40}	204	701	802	274
$\overline{F_{87} - F_{78}}$	25.0	25.0	25.0	25.0
F_{X3}	1901	1108	1128	1414
F_{X4}	140	513	523	188
F_{X7}	502	419	465	437
F_{73}	866	405	602	650
F_{74}	63.9	188	279	86.4
$F_{07}^{(s)}$	1128	708	1098	936
F_{06}	1259	827	2647	1686
F_{70}	942	674	884	752
F_{76}	434	225	395	321

intracellular pools, in particular flows F_{06}, F_{60},$F_{07}^{(s)}$ and F_{70} representing constitutive protein synthesis and degradation and flows F_{96}, F_{X7}, F_{73}, representing movement of PHE and TYR out of and into the intracellular pools. Therefore, to assess the differences in calculated flows between the combined model of Crompton *et al.* (2018) and the split model described herein, a sensitivity analysis was undertaken to examine the effect of varying experimental enrichments and infusion rates on model solutions. Input data in Table 2 and inputs reported by Crompton *et al.* (2018) were averaged to provide initial unperturbed values for e_1, e_2, e_6, e_9, ε_3, ε_4, ε_7, ε_x, I_1, I_2, Φ_3, Φ_4, F_{05}, $F_{07}^{(o)}$, F_{08}, F_{09}, F_{0X}. Inputs to the split model were perturbed sequentially by 0, ±10% and ±20%. The perturbed input (x, %), was plotted against each calculated flow (y, μmol/min) and a linear five-point regression of y on x performed to determine the slope of the line produced. The average slope was subsequently scaled by its corresponding unperturbed average flow value, giving the scaled slopes dimensions of % change in y per % change in x. Results of the sensitivity analysis are presented in Table 5. In general, errors in infusion rates and prescribed flows had less impact on the sensitivity of model solutions than errors in the measurement of isotopic enrichment and in assumed intracellular enrichment values. Measuring intracellular enrichment directly would require a sample of liver tissue at the end of the isotope infusion (e.g. Connell *et al.*, 1997).

Discussion

Increasing the efficiency of conversion of feed N into milk and meat N in ruminant production is an integral part of the effort to increase global food production while decreasing agriculture's environmental impact (Dijkstra *et al.*, 2018; Grossi *et al.*, 2018). Improving N utilization in the ruminant is dependent on a clear understanding of post-absorptive amino acid metabolism (Reynolds, 2006). The present model described the partitioning of the indispensable amino acid PHE (and TYR) in the bovine liver and provided estimates of PHE and TYR flow across the liver, rates of PHE and TYR incorporation into constitutive and export protein synthesis, and the rate of hydroxylation of PHE to TYR. The scheme presented herein (Fig. 1) and evaluated for dairy cows should be readily applicable to other mammals and birds, including farm livestock, pets and humans.

PHE and TYR enter the liver via the portal vein, the main blood supply to liver, and the hepatic artery. Amino acids in the portal vein represent recently absorbed or released amino acids from the portal drained viscera and amino acids present in the mesenteric arterial supply. The total flow of amino acids in the arterial supply to the portal-drained viscera is considerably greater than the amount added by absorption and any net uptake by the same tissues. Amino acids in hepatic and mesenteric arterial blood reflect the impact of peripheral tissue nutrient utilization on amino acid availability in the arterial pool (Reynolds, 2006).

https://doi.org/10.1017/S0021859622000442 Published online by Cambridge University Press

Table 4. Phenylalanine and tyrosine uptake and partition by the liver of lactating dairy cows obtained using the two five-pool models (symbols are defined in the text and Table 1) and the corresponding solutions obtained using the ten-pool model of Crompton *et al.* (2018)

Model	Two 5-pool models solution	10-pool model solution
Flow (μmol/min)		
F_{10}	2450 (256)	2450 (256)
F_{20}	599 (133.1)	599 (133.1)
$\overline{F_{56} - F_{65}}$	33.8	33.8
F_{91}	1701 (180)	1763 (185)
F_{92}	416 (90.8)	430 (93.0)
F_{96}	409 (46.6)	334 (36.1)
F_{61}	749 (88.3)	688 (78.3)
F_{62}	184 (44.7)	170 (41.0)
F_{60}	1240 (152)	2197 (402)
F_{30}	1954 (191)	1954 (191)
F_{40}	490 (85.8)	490 (85.8)
$\overline{F_{87} - F_{78}}$	25.0	25.0
F_{X3}	1358 (132)	1443 (139)
F_{X4}	339 (58.1)	345 (60.5)
F_{X7}	433 (37.9)	342 (35.3)
F_{73}	596 (62.4)	511 (61.0)
F_{74}	151 (28.7)	144 (30.3)
$F_{07}^{(s)}$	986 (117.9)	1808 (156)
F_{06}	1468 (204)	2447 (451)
F_{70}	837 (90.5)	1681 (129)
F_{76}	261 (45.8)	239 (46.9)

Values are means across data sets (both those reported here and those reported by Crompton *et al.* (2018)). Figures in parentheses are standard error of the mean.

The model demonstrated a greater flow of PHE and TYR from the portal vein (80% of total inflow) than that from the hepatic artery, which was expected as the portal vein accounted for the majority (75%) of liver blood flow in the four animals. *In vivo* studies have observed a negative net flow (net removal) of PHE across the bovine liver, suggesting the liver is a major site of catabolism (e.g. Larsen *et al.*, 2015). In agreement, model solutions indicated a net negative flow of PHE and TYR across the liver (outflow minus inflow, −651 and −329 μmol/min PHE and TYR respectively).

Within the liver PHE may either be used for protein synthesis or be converted to TYR, the conversion of which is catalysed by PHE hydroxylase. TYR is not considered essential, because it can be synthesized from PHE in addition to that provided by the diet. On average the model estimated that 36% of inflow of PHE from blood (sum of hepatic artery and portal vein inflows) to the liver was converted to TYR. Outflows of PHE and TYR from the liver include oxidation and incorporation into secreted hepatic proteins. Oxidation rates varied greatly in individual animals (range 339–650 μmol/min), the lowest value observed in the animal receiving the water infusion and in our previous work the highest rate of oxidation (525 μmol/min) was observed in the one animal receiving the essential amino acid infusion (Crompton *et al.*, 2018). Higher rates of oxidation in animals receiving additional PHE via the essential amino acid infusions reflect an increased supply relative to requirements. The oxidation rate in the animal receiving the control water infusion was similar to those previously reported in lactating dairy cows fed a high protein diet (Raggio *et al.*, 2007). Oxidation rates used in the present model accounted for 28% of total PHE and TYR inflow to the liver. Measuring TYR oxidation directly represents a challenge experimentally. In general, deuterium labelled PHE is inadequate for quantifying PHE kinetics and oxidation, which requires the use of carbon labelled PHE and by default, deuterium labelled TYR (Matthews, 2007).

The liver makes several export proteins of various functions. Albumin is important for the maintenance of intravascular colloid osmotic pressure. Due to this critical role, albumin synthesis is maintained across various mild physiological challenges, although in more severe situations of nutrient shortage, albumin synthesis may decrease. Raggio *et al.* (2007) determined export plasma protein synthesis rate in lactating dairy cows and assumed that export plasma protein contained 5% PHE. The value thus obtained was used in the present model to represent the flow of PHE into export protein. Since plasma proteins are also derived from sources other than the liver, the assumption that total plasma export protein synthesis is all hepatic in origin might overestimate the flow of PHE into export protein in the current model, however, given export protein PHE flow is minor (33.8), overestimation will have negligible impact on other PHE flows. The incorporation of TYR into albumin was unknown and assumed equivalent to that of PHE after correcting for the relative proportions of PHE and TYR in albumin. This assumption is recognized as a limitation of the current modelling exercise. Specifically, the incorporation of individual amino acids depends on the type of export protein; some export proteins may require proportionally higher or lower amounts of PHE or TYR.

Model solutions representing the rate of constitutive protein synthesis for PHE and TYR enable the ratio of PHE:TYR in constitutive liver protein to be estimated. The ratio was variable and ranged from 1.1 to 2.4. with a mean value of 1.63, this compares with a mean of 1.30 (range 1.06–1.66) using the ten-pool solution (Crompton *et al.*, 2018) and are comparable to the ratio calculated from the measured amino acid composition of calf liver of 1.36 (range 1.22–1.43) reported by Rius *et al.* (2012).

A feature of the present model is the description of intracellular PHE and TYR partitioning. Constitutive hepatic protein degradation, for example, was a larger contributor to the free PHE and TYR pools than portal vein and hepatic artery delivery, with delivery being 76 and 96% of degradation in the case of PHE and TYR, respectively. Model estimates of intracellular PHE and TYR partitioning must be interpreted with caution due to methodological limitations and imposed assumptions. For example, samples were taken from whole blood and free PHE and TYR concentrations were quantified and considered in the model. Therefore, the extent to which peptide-bound PHE and TYR contribute to constitutive protein synthesis and degradation flows cannot be determined. As hepatic tissues were not sampled, isotopic enrichment of the intracellular pools was estimated based on the sampled precursor pools. The choice of precursor pool enrichment is central in the present model as with any measurement of protein synthetic rate in the whole body or tissues (Waterlow, 2006). The assumption that intracellular enrichments were 0.30 of plasma was based on unpublished

https://doi.org/10.1017/S0021859622000442 Published online by Cambridge University Press

Table 5. Average slope (%) for each of the flows calculated by the model obtained by perturbing each input in turn[a]

	Unperturbed	Input perturbed[b]																
Flow	(μmol/min)[c]	e_1	e_2	e_6	e_9	ε_3	ε_4	ε_7	ε_X	I_1	I_2	Φ_3	Φ_4	F_{05}	$F_{07}^{(o)}$	F_{08}	F_{09}	F_{0X}
F_{10}	2472									1.0								
F_{20}	635										1.0							
$\overline{F_{56} - F_{65}}$	33.8													1.0				
F_{91}	1693	−1.3	−0.51	−0.16	1.9					0.36	−0.36						1.0	
F_{92}	435	−1.3	−0.51	−0.16	1.9					−0.65	0.65						1.0	
F_{96}	456	6.1	2.4	0.76	−8.9					−0.72	0.71						1.0	
F_{61}	779	2.8	1.1	0.35	−4.1					2.4	0.78						−2.2	
F_{62}	200	2.8	1.1	0.35	−4.1					1.4	1.8						−2.2	
F_{60}	1311	3.9	1.6	−1.4	−4.1					2.0	1.1						−2.2	
F_{30}	1936											1.0						
F_{40}	527												1.0					
$\overline{F_{87} - F_{78}}$	25.0															1.0		
F_{X3}	1357					−1.3	−0.50	−0.17	1.9			0.35	−0.35					1.0
F_{X4}	370					−1.3	−0.50	−0.17	1.9			−0.66	0.66					1.0
F_{X7}	428					5.1	2.0	0.70	−7.5			−0.54	0.53					1.0
F_{73}	579					3.0	1.2	0.41	−4.4			2.5	0.8					−2.3
F_{74}	158					3.0	1.2	0.41	−4.4			1.6	1.8					−2.3
$F_{07}^{(s)}$	985				0.38	4.3	1.8	−1.4	−4.7			4.3	1.8		−0.37	−0.03		−4.7
F_{06}	1561	3.6	1.4	−1.3	−3.7	−0.31	−0.12	0.09	0.34	2.8	1.3	0.57	0.10	−0.01	−0.13	−0.01	−3.0	−0.66
F_{70}	827	0.52	0.18	−0.15	−0.34	4.6	1.9	−1.5	−5.0	−0.91	−0.15	3.9	1.7	0.01	−0.24	−0.02	1.0	−4.3
F_{76}	239	−1.8	−0.61	0.51	1.2	2.0	0.78	−0.61	−2.2	3.1	0.52	−3.7	−0.68	−0.05	0.84	0.06	−3.3	4.3

[a]The slope for each flow is expressed relative to the value of the flow obtained when no perturbation is made. Only slopes which differ from zero are shown
[b]Model solved by perturbing each input in turn by 0, ±10 and ±20%
[c]Values calculated from the mean of inputs reported in Table 2 and inputs reported by Crompton *et al.* (2018)

observations from an unrelated *in vivo* trial from our laboratory. Using the same isotopes as the present study, average liver homogenate-free enrichment for PHE and TYR was 0.30 (S.D. 0.07; range 0.19–0.38) of plasma enrichment in lactating dairy cattle. Besides, the actual precursor pool for various constitutive and export proteins may differ. Lack of homogeneity in activity at various parts of the liver indicates that intracellular enrichment is not uniform throughout the liver, and enrichment in export protein and constitutive protein therefore may differ. In particular, the precursor enrichment for constitutive protein synthesis may be lower than that for export protein synthesis (Connell *et al.*, 1997). Due to the lack of specific measurements, export protein precursor enrichment could not be included in the present model.

The two sub-models described herein are based on compartmental analysis and isotope tracer methods for kinetic studies *in vivo*. Conservation of mass principles are applied to each pool to generate differential equations which describe the behaviour of the system in steady state. This is the same approach as used in our previous work on amino acid uptake by the bovine liver (France *et al.*, 1999; Crompton *et al.*, 2018). However, splitting the original 10-pool model reduces the number of interlinked pools and the number of unknowns within each scheme. Solving the PHE and TYR sub-models sequentially, then linking the two solutions algebraically to re-create the integrated model, eliminates the necessity of having to use [^{13}C]TYR enrichment in pools 3, 4, 6 and *X* for model solution. Enrichment of [^{13}C]TYR was on average only 12% of the corresponding [^{13}C]PHE enrichment and was close to minimum detection levels. Sensitivity analysis of model solutions has shown that measured isotopic enrichment and assumed intracellular enrichment values have the greatest impact on calculated flows, highlighting the importance of precise isotopic enrichment analysis and measuring intracellular enrichment directly. Solving the original model as two five-pool schemes yielded biologically feasible solutions, i.e. the computed flows were all non-negative, consequently there was no requirement to map the solution space iteratively with error bands of ±25% for prescribed intracellular and measured extracellular enrichments to find best feasible solutions as for the ten-pool model (Crompton *et al.*, 2018). Solving the model by cleaving into two five-pool schemes rather than solving the ten-pool scheme directly is therefore preferred as there appears to be less compounding of errors. Accurate values of the intracellular and extracellular enrichments are central to minimising errors in the calculated flows.

Conclusion

Herein, a ten-pool model of liver PHE and TYR metabolism was solved by cleaving into two five-pool sub-models (one for PHE and one for TYR), solving them separately, and linking the two solutions by assuming the ratios of TYR to PHE in protein synthesized and protein degraded are equal. The sensitivity analysis conducted on enrichments, infusion rates and prescribed flows indicated model solutions were most sensitive to values of the enrichments. Previously, the model was solved as a single ten-pool scheme (Crompton *et al.*, 2018). Initial solutions for each of the cows reported were non-physiological as some of the derived flows gave negative values. The solutions reported herein derived using two five-pool schemes without the use of iteration were biologically feasible, i.e. the computed flow values are all non-negative. Solving the model by cleaving into two five-pool schemes rather than solving the ten-pool scheme directly is therefore preferred as there appears to be less compounding of errors. Accurate values of the intracellular and extracellular enrichments are central to minimising errors in the calculated flows.

Author contributions. Conceptualization: LAC, CKR and JF; methodology: LAC, CKR, JD and JF; formal analysis: LAC, LAM, JLE and JF; writing – original draft preparation: LAC and JF; writing – review and editing: LAC, LAM, CKR, JLE, JD and JF. All authors have read and agreed to the published version of the manuscript.

Financial support. This work was funded, in part, through DEFRA project LS3656 and the Canada Research Chairs Program. The experimental work was funded by a consortium of DEFRA, BBSRC, the Milk Development Council, Purina Mills LLC and NUTRECO Inc.

Conflict of interest. None.

Ethical standards. All experimental procedures used were licensed, regulated and inspected by the UK Home Office under the Animals (Scientific Procedures) Act, 1986.

References

Cantalapiedra-Hijar G, Lemosquet S, Rodriguez-Lopez JM, Messad F and Ortigues-Marty I (2014) Diets rich in starch increase the post-hepatic availability of amino acids in dairy cows fed diets at low and normal protein levels. *Journal of Dairy Science* **97**, 5151–5166.

Connell A, Calder AG, Anderson SE and Lobley GE (1997) Hepatic protein synthesis in the sheep: effect of intake as monitored by use of stable-isotope-labelled glycine, leucine and phenylalanine. *British Journal of Nutrition* **77**, 255–271.

Crompton LA, McKnight LL, Reynolds CK, Mills JAN, Ellis JL, Hanigan MD, Dijkstra J, Bequette BJ, Bannink A and France J (2018) An isotope dilution model for partitioning phenylalanine and tyrosine uptake by the liver of lactating dairy cows. *Journal of Theoretical Biology* **444**, 100–107.

Crompton LA, McKnight LL, Reynolds CK, Ellis JL, Dijkstra J and France J (2022) Further solutions to an isotope dilution model for partitioning phenylalanine and tyrosine between milk protein synthesis and other metabolic fates by the mammary gland of lactating dairy cows. *Journal of Agricultural Science*, 1–10. https://doi.org/10.1017/S0021859622000223.

Dijkstra J, Reynolds CK, Kebreab E, Ellis JL, France J and van Vuuren AM (2013) Challenges in ruminant nutrition: towards minimal nitrogen losses in cattle. In Proceedings of the 4th International Symposium on Energy and Protein Metabolism (Eds Oltjen JW, Kebreab E and Lapierre H), EAAP Publ. No. 134, pp. 47–58. Wageningen, the Netherlands: Wageningen Academic Publishers.

Dijkstra J, Bannink A, Bosma PM, Lantinga EA and Reijs JW (2018) Modelling the effect of nutritional strategies for dairy cows on the composition of excreta nitrogen. *Frontiers in Sustainable Food Systems* **2**, 63.

Doepel L, Hewage II and Lapierre H (2016) Milk protein yield and mammary metabolism are affected by phenylalanine deficiency but not by threonine or tryptophan deficiency. *Journal of Dairy Science* **99**, 3144–3156.

France J, Hanigan MD, Reynolds CK, Dijkstra J, Crompton LA, Maas JA, Bequette BJ, Metcalf JA, Lobley GE, MacRae JC and Beever DE (1999) An isotope dilution model for partitioning leucine uptake by the bovine liver. *Journal of Theoretical Biology* **198**, 121–133.

Grossi G, Goglio P, Vitali A and Williams AG (2018) Livestock and climate change: impact of livestock on climate and mitigation strategies. *Animal Frontiers* **9**, 69–76.

Hanigan MD, Crompton LA, Reynolds CK, Wray-Cahen D, Lomax MA and France J (2004) An integrative model of amino acid metabolism in the liver of the lactating dairy cow. *Journal of Theoretical Biology* **228**, 271–289.

Harris PA, Skene PA, Buchan V, Milne E, Calder AG, Anderson SE, Connell A and Lobley GE (1992) Effect of food intake on hind-limb and whole-body protein metabolism in young growing sheep: chronic studies based on arterio-venous techniques. *British Journal of Nutrition* **68**, 389–407.

Hristov AN, Bannink A, Crompton LA, Huhtanen P, Kreuzer M, McGee M, Nozière P, Reynolds CK, Bayat AR, Yáñez-Ruiz DR, Dijkstra J, Kebreab

E, Schwarm A, Shingfield KJ and Yu Z (2019) Nitrogen in ruminant nutrition: a review of measurement techniques. *Journal of Dairy Science* **102**, 5811–5852.

Larsen M, Galindo C, Ouellet DR, Maxin G, Kristensen NB and Lapierre H (2015) Abomasal amino acid infusion in postpartum dairy cows: effect on whole-body, splanchnic, and mammary amino acid metabolism. *Journal of Dairy Science* **98**, 7944–7961.

Matthews DE (2007) An overview of phenylalanine and tyrosine kinetics in humans. *Journal of Nutrition* **137**, 1549S–1555S.

Nichols K, Bannink A and Dijkstra J (2019) Energy and nitrogen balance of dairy cattle as affected by provision of different essential amino acid profiles at the same metabolizable protein supply. *Journal of Dairy Science* **102**, 8963–8976.

Raggio G, Lobley GE, Berthiaume R, Pellerin D, Allard G, Dubreuil P and Lapierre H (2007) Effect of protein supply on hepatic synthesis of plasma and constitutive proteins in lactating dairy cows. *Journal of Dairy Science* **90**, 352–359.

Reynolds CK (2002) Economics of visceral nutrient metabolism in ruminants – toll keeping or internal revenue service? *Journal of Animal Science* **80**(E Suppl. 2), E74–E84.

Reynolds CK (2006) Splanchnic metabolism of amino acids in ruminants. In Sejrsen K, Hvelplund T and Nielsen MO (eds), *Ruminant Physiology: Digestion, Metabolism and Impact of Nutrition on Gene Expression, Immunology and Stress*. Wageningen, the Netherlands: Wageningen Academic Press, pp. 225–248.

Rius AG, Weeks HA, Cyriac J, Akers RM, Bequette BJ and Hanigan MD (2012) Protein and energy intakes affected amino acid concentrations in plasma, muscle, and liver, and cell signalling in the liver of growing dairy calves. *Journal of Dairy Science* **95**, 1983–1991.

Rulquin H and Pisulewski P (2000) Effects of duodenal infusions of graded amounts of Phe on mammary uptake and metabolism in dairy cows. *Journal of Dairy Science* **83**(Suppl. 1), 267–268.

UniProt Consortium (2017) UniProt: the universal protein knowledgebase. *Nucleic Acids Research* **45**, D158–D169.

Uwizeye A, de Boer IJM, Opio CI, Schulte RPO, Falcucci A, Tempio G, Teillard F, Casu F, Rulli M, Galloway JN, Leip A, Erisman JW, Robinson TP, Henning Steinfeld H and Gerber PJ (2020) Nitrogen emissions along global livestock supply chains. *Nature Food* **1**, 437–446.

Waterlow JC (2006) *Protein Turnover*. Wallingford, UK: CAB International.

https://doi.org/10.1017/S0021859622000442 Published online by Cambridge University Press